The prognostic importance of the negative regulators of ferroptosis, GPX4 and HSPB1, in patients with colorectal cancer

TADANOBU SHIMURA[1], CHENGZENG YIN[1], RUIYA MA[1,2], AIYING ZHANG[1], YUKA NAGAI[1], AOI SHIRATORI[1], HANA OZAKI[1], SHINJI YAMASHITA[1], KOKI HIGASHI[1], YUKI SATO[1], HIROKI IMAOKA[1], TAKAHITO KITAJIMA[1,3], MIKIO KAWAMURA[1], YUHKI KOIKE[1], YOSHIKI OKITA[1], SHIGEYUKI YOSHIYAMA[1], MASAKI OHI[1], AKINOBU HAYASHI[4], HIROSHI IMAI[4], XUEMING ZHANG[2], YOSHINAGA OKUGAWA[1,3] and YUJI TOIYAMA[1]

[1]Department of Gastrointestinal and Pediatric Surgery, Institute of Life Sciences, Mie University Graduate School of Medicine, Tsu, Mie 514-8507, Japan; [2]Department of Surgery, Tangshan Gongren Hospital, Tangshan, Hebei 063007, P.R. China; [3]Department of Genomic Medicine, Mie University Hospital, Tsu, Mie 514-8507, Japan; [4]Department of Oncologic Pathology, Mie University Graduate School of Medicine, Tsu, Mie 514-8507, Japan

Received September 16, 2024; Accepted December 16, 2024

DOI: 10.3892/ol.2025.14890

Abstract. The prognostic value of negative regulators of ferroptosis in patients with colorectal cancer (CRC) has not yet been fully elucidated. The present study performed a systematic *in silico* identification and selection of candidate negative regulators of ferroptosis using The Cancer Genome Atlas data cohort (n=367), followed by clinical validation through immunohistochemistry of samples from patients with CRC (n=166) and further *in vitro* evaluation. *In silico* analysis identified specific light-chain subunit of the cystine/glutamate antiporter, AIFM2, NFE2L2, FTH1, GLS2, glutathione peroxidase 4 (GPX4) and heat shock protein β-1 (HSPB1) genes as possible candidates. Furthermore, patients with high expression of GPX4 or HSPB1 exhibited significantly worse overall survival (OS) compared with those with low expression (P<0.01 for both). Immunohistochemical analysis revealed that both OS and recurrence-free survival (RFS) of patients with CRC and high GPX4 or HSPB1 expression were significantly worse compared with in patients with low expression (P<0.01 for all). Furthermore, multivariate analysis showed that high GPX4 and HSPB1 expression were independent risk factors for poor oncological outcome for OS and RFS (GPX4: RFS, P=0.03; HSPB1: OS, P=0.006 and RFS, P<0.0001). Moreover, the effects of GPX4 and HSPB1 small interfering RNAs on two CRC cell lines (DLD-1 and SW480) indicated that GPX4 and HSPB1 may exhibit important roles in attenuating the cytotoxic effect of 5-fluorouracil-based chemotherapy. In conclusion, the current study confirmed that GPX4 and HSPB1 may serve as substantial prognostic- and recurrence-predictive biomarkers in patients with CRC.

Correspondence to: Dr Tadanobu Shimura, Department of Gastrointestinal and Pediatric Surgery, Institute of Life Sciences, Mie University Graduate School of Medicine, 2-174 Edobashi, Tsu, Mie 514-8507, Japan
E-mail: tadanobu189222@gmail.com

Abbreviations: CRC, colorectal cancer; GPX4, glutathione peroxidase 4; HSPB1, heat shock protein β-1

Key words: CRC, ferroptosis, HSPB1, GPX4, prognostic biomarker

Introduction

Colorectal cancer (CRC) is one of the leading causes of cancer-associated death worldwide (1). While multidisciplinary treatment for CRC, including surgery, neoadjuvant chemoradiotherapy, postoperative chemoradiotherapy, chemotherapy (including molecular targeted therapy), and immunotherapy, has decreased the risk of recurrence and improved survival and outcomes (2-4), the 5-year survival rates of CRC patients are still not satisfactory, in part because of multidrug resistance and cancer progression (5-8).

The high mortality rate of CRC is mainly from late disease diagnosis and lack of adequate prognostic biomarkers. While treatment recommendations and prognosis prediction of CRC patients are determined using the tumor-node-metastasis (TNM) classification system (9), CRC exhibits heterogeneity, and even same-stage individuals can show different clinical outcomes and response to treatment (10). Thus, the identification of robust prognostic markers is critical. Moreover, such biomarkers possess adequate prognostic significance for specific subgroups decided by the TNM staging system (11).

Ferroptosis, which was first discovered in 2012, is a newly defined form of programmed cell death distinct from apoptosis, necrosis, and autophagy (12). Ferroptosis is characterized by iron accumulation, lipid peroxidation, and accumulation of lipid reactive oxygen species (ROS) within cells. Ferroptosis is distinct from other types of regulated cell death in various aspects (12,13). For example, ferroptotic cells show unique biochemical, morphological, and genetic features, such as

ruptured cellular membrane, lack of chromatin condensation, shrunken mitochondria, and increased density of the mitochondrial membrane (14). Several studies have shown that ferroptosis is involved in various diseases and processes, including neurodegeneration, neurotoxicity, drug-induced hepatotoxicity, acute renal failure, tissue ischemia/reperfusion, immunological abnormality, and carcinogenesis (15-18).

Reports have also shown that therapy-resistant cancer cells are sensitive to ferroptosis, suggesting that targeting ferroptosis could be a promising strategy for cancer (19). We previously demonstrated that some botanical compounds that possess anti-tumorigenic potential altered the expression of ferroptosis-related genes; the compounds induced suppression of cancer progression and restored chemosensitivity in gastrointestinal cancer (20-22). We thus hypothesized that negative regulators of ferroptosis may also have a role in CRC development.

Ferroptosis is negatively regulated by limiting ROS production and reducing cellular iron uptake. Negative regulation of ferroptosis is mediated by glutathione peroxidase 4 (GPX4), heat shock protein β-1 (HSPB1), nuclear factor erythroid 2-related factor 2 (NRF2), and specific light-chain subunit of the cystine/glutamate antiporter (SLC7A11) (23). The association between the expression of negative regulators of ferroptosis and the oncological outcome of CRC patients has not been examined.

In this study, we conducted a systematic investigation to first identify candidate ferroptosis negative regulator genes that may be associated with the prognosis of CRC patients by *in silico* analysis. We then confirmed the clinical importance of candidate genes as prognostic biomarkers by validation using clinical specimens from CRC patients.

Materials and methods

Study design. The present study consisted of a search for negative regulators of ferroptosis through *in silico* testing and validation in clinical samples of CRC patients. The study flow is shown in Fig. 1A. Details on the discovery phase and gene identification are described below.

Patient characteristics. Stage 1 to stage 4 CRC patients (n=166) who underwent surgical resection at the Department of Gastrointestinal and Pediatric Surgery of the Mie University Graduate School of Medicine from January 2012 to December 2015 were enrolled in this study. Patients with incomplete clinical data or inadequate immunohistochemistry (IHC) results were excluded. Patient clinicopathological characteristics are shown in Table SI. Staging was performed on the basis of clinical and histopathological assessment following the International Union Against Cancer TNM staging system (24). All patients were followed up after initial hospital discharge, with physical examination and tumor marker assays (CEA and CA19-9) performed every 1-3 months and computed tomography every 6 months; endoscopic examinations were performed when necessary. Written informed consent was obtained from all patients following the local ethics guidelines, and the Institutional Review Board (IRB) of Medical Ethics Committee of Mie University Graduate School of Medicine approved this study (IRB number: H2023-172).

Comprehensive in silico analysis of negative regulators of ferroptosis. Several studies have discussed genes associated with negative regulation of ferroptosis (23,25-29). In this study, we confirmed the candidate ferroptosis negative regulator genes using the Gene Ontology Consortium Website (www.geneontology.org, and http://www.informatics.jax.org/vocab/gene_ontology/). We downloaded gene expression from the RNAseq (IlluminaHiSeq) dataset of 'The Cancer Genome Atlas (TCGA) Colon and Rectal Cancer (COADREAD)' patients (https://xenabrowser.net/datapages/). We investigated the association between the expression profile of seven ferroptosis negative regulator genes, SLC7A11, AIFM2, NFE2L2 (NRF2), FTH1, GLS2, GPX4, and HSPB1, and overall prognosis in the 367 CRC patients in the *in silico* cohort with available survival data.

IHC. Formalin-fixed, paraffin-embedded sections (5 μm thickness) of specimens from the 166 CRC patients were subjected to immunohistochemical analysis. After deparaffinization by xylene and rehydration in graded concentrations of ethanol, specimens were heated at 121˚C for 10 min in citrate buffer (pH 6.0) to unmask antigens. Endogenous peroxidase activity was blocked by incubation with 3% hydrogen peroxide in distilled water. Nonspecific binding sites were blocked with 10% normal goat serum (Vector Laboratories, Burlingame, CA, USA) in Tris-buffered saline with 0.05% Tween 20 (TBST), and samples were incubated with primary antibody overnight at 4˚C. Primary GPX4 antibody (Abcam, Waltham, MA, USA) was used at 1:1,000, and primary HSPB1 antibody (same as HSP27, Santa Cruz Biotechnology, Dallas TX, USA) was used at 1:1,000. After washing with TBST, sections were incubated with secondary antibody coupled with peroxidase-conjugated polymers [Universal Immuno-peroxidase Polymer method, Histofine SAB-PO(M) Kit, Nichirei Biosciences, Inc., Tokyo, Japan] for 30 min and detected using the Histofine DAB substrate kit (Nichirei Biosciences, Inc.). Slides were counterstained with hematoxylin, as previously described (30-33).

Evaluation of immunohistochemical staining. GPX4 and HSPB1 expression of CRC specimens were analyzed three times separately by two investigators who were not familiar with the clinical or survival data of patients. The investigators first evaluated the entire tissue specimen at low-power magnification (x40) and then focused on tumor hotspots at high-power magnification (x200 and x400). As previously described (30-33), an immunohistochemical score was determined for each case as follows: Staining intensity score: 0, colorless; 1, weak; 2, moderate; and 3, strong; and staining percentage score: 1, 1-25; 2, 26-50; 3, 51-75 and 4, >75% positivity. The IHC score of each patient was obtained by multiplying the scores for staining intensity and staining percentage. If the difference between the scores obtained from each investigator was >3, the stained slide was reassessed.

Cell culture and materials. CRC cell lines (DLD-1, RKO, SW480, and LOVO) were acquired from the Cell Resource Center of Biomedical Research, Institute of Development, Aging and Cancer (Tohoku University; Sendai, Japan). The CRC cells were maintained in RPMI 1640 (Nacalai Tesque Inc., Kyoto, Japan), supplemented with 10% fetal bovine serum

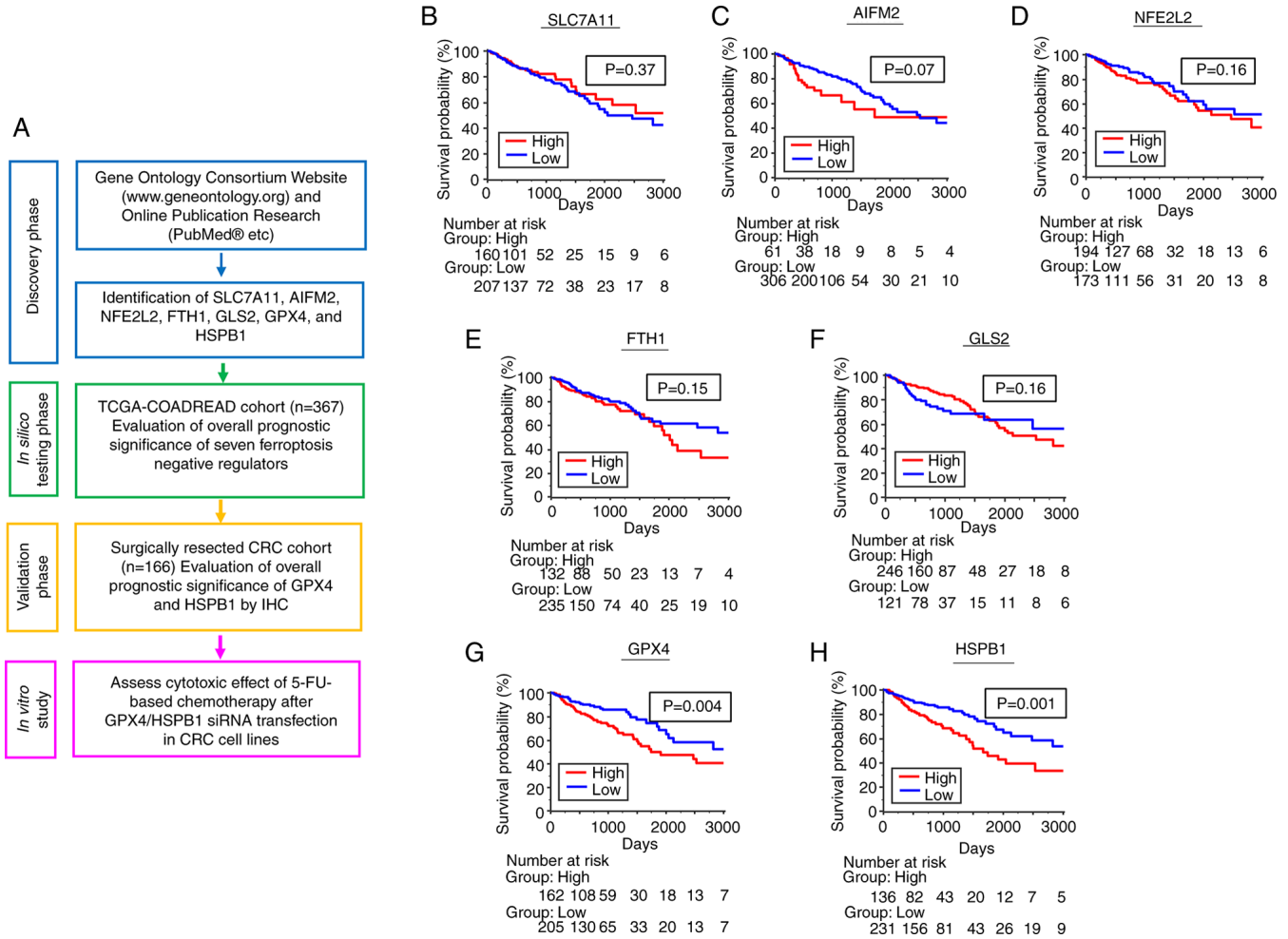

Figure 1. Identification and *in silico* evaluation of candidate ferroptosis negative regulators for prognostic biomarkers in CRC patients. (A) Schematic of the project flow. Kaplan-Meier analysis of OS in patients with CRC from TCGA cohort according to the following individual candidate ferroptosis negative regulators: (B) SLC7A11, (C) AIFM2, (D) NFE2L2, (E) FTH1, (F) GLS2, (G) GPX4 and (H) HSPB1. CRC, colorectal cancer; OS, overall survival; TCGA-COADREAD, The Cancer Genome Atlas-Colon and Rectal Cancer; 5FU, 5-fluorouracil; siRNA, small interfering RNA.

(FBS, Biowest, Nouille, France) and Antibiotic-Antimycotic (Nacalai Tesque Inc.) and maintained at 37˚C in a humidified incubator at 5% CO_2. All cell lines were checked and authenticated using a panel of genetic and epigenetic markers and tested for mycoplasma on a regular basis. 5-Fluorouracil (5FU, Sigma-Aldrich, MA, USA) was dissolved in dimethyl sulfoxide and diluted to the appropriate experimental concentrations in cell culture medium before use.

RNA interference. Specific predesigned small interfering RNA (siRNA) for GPX4 and HSPB1 and Negative Control siRNA were purchased from Ambion (Thermo Fisher Scientific, Inc., USA). The siRNA sequences of GPX4 and HSPB1 were as follows: GPX4: sense, 5'-GGCAAGACCGAAGUAAACUtt-3' and antisense, 5'-AGUUUACUUCGGUCUUGCCtc-3'; and HSPB1: sense, 5'-CGAGAUCACCAUCCCAGUCtt-3' and antisense, 5'GACUGGGAUGGUGAUCUC Gtt-3' (SiRNA ID number for GPX4 is 10848, and for HSPB1 is 121323. Catalogue number for Negative Control siRNA is 4390843). We used two CRC cell lines (DLD-1 and SW480) with high gene expression of GPX4 and HSPB1 for experiments. DLD-1 and SW480 cells were seeded in six-well culture plates at $2x10^5$ cells per well in 2 ml RPMI 1640. Cells were cultured for 24 h and then incubated with siRNA oligonucleotides using Lipofectamine RNAiMAX Reagent and OptiMEM I (both Invitrogen, Thermo Fisher Scientific, Inc.) following the manufacturer's protocol. The final concentration of siRNA oligonucleotide of GPX4/HSPB1 was 50 nM. After 48 h, transfected cells were harvested and examined by RT-qPCR and western blotting to check siRNA efficiency.

Total RNA extraction and cDNA synthesis. Total RNA was extracted from CRC cell lines (DLD1, RKO, SW480, and LOVO) using miRNeasy (Qiagen, Germany) following the manufacturer's instructions. RNA quality and concentration were determined using a Denovix DS-11+ spectrophotometer (DeNovix, Inc., USA). cDNA was synthesized from 5 μg of total RNA with random hexamer primers, dNTPs, 5X buffer, RNase inhibitor, and ReverTra Ace (Toyobo Co., LTD., Japan).

Reverse transcription-quantitative PCR (RT-qPCR). RT-qPCR analyses were conducted using the SYBR Green PCR Master Mix and QuantStudio3 Real-Time PCR System (Applied Biosystems, Thermo Fisher Scientific, Inc., USA) following the manufacturer's protocol and as previously described (22). The qPCR cycling conditions were as follows: 95˚C for

10 min, followed by 45 cycles of 15 sec at 95˚C and 60 sec at 60˚C. Primers for GPX4, HSPB1 and GAPDH mRNAs were as follows; GPX4: forward, 5'-GAGGCAAGACCGAAG TAAACTAC-3' and reverse, 5'-CCGAACTGGTTACACGGG AA-3'; HSPB1: forward, 5'-ACGGTCAAGACCAAGGAT GG-3' and reverse, 5'-AGCGTGTATTTCCGCGTGA-3'; and GAPDH: forward, 5'-GGAAGGTGAAGGTCGGAGTC-3' and reverse, 5'-AATGAAGGGGTCATTCATGG-3'. Relative expression levels of GPX4 and HSPB1 mRNA were calculated by normalization to the levels of endogenous GAPDH mRNA using the $2^{-\Delta\Delta Cq}$ method (22). RT-qPCR assays were performed in triplicate for each sample and the mean value was calculated.

Western blotting. At 48 h after transfection of GPX4 or HSPB1 siRNA, cells were lysed in RIPA buffer (BioDynamics Laboratory, Inc., Tokyo, Japan) with protease inhibitors, and lysates were centrifuged for 5 min at 15,000 x g at 4˚C. The protein concentration was measured using the BCA protein assay kit (Thermo Fisher Scientific, Inc.). Protein samples (20 μg) were separated on AnykD™ Mini-PROTEAN® TGX™ Precast Protein Gels and then transferred onto a polyvinylidene difluoride membrane (Bio-Rad Laboratories, CA, USA). The blots were first blocked with 5% skimmed milk for 1 h at room temperature and then incubated overnight with primary antibodies against GPX4 (1:20,000; Abcam, Cambridge, UK), HSPB1 (1:10,000; Santa Cruz, CA, USA), and β-actin (1:40,000; MP Biomedicals, Illkirch, France). The blots were incubated with secondary antibody (Promega, Madison, WI, USA) for 60 min at room temperature. The protein bands were visualized by chemiluminescent reaction (Immobilon™ Western; Millipore, MA, USA) coupled with a WSE-6100 LuminoGraph imaging system (ATTO Corporation, Tokyo, Japan).

Cell viability assay. After transfection of GPX4 or HSPB1 siRNA, DLD-1 and SW480 cells were plated in 96-well tissue culture plates (TPP Techno Plastic Products AG, Switzerland) at a density of 3,000 cells/well in RPMI1640 medium supplemented with 10% FBS and antibiotics. The cells were allowed to adhere to the plate for 24 h and then treated with a series of two-fold dilution of 5FU (0, 6.25, 12.5, 25, 50, 100, 200, 400 μM). After 72 h of treatment, cell proliferation was measured using the WST8 assay (Dojindo Laboratories, Kumamoto, Japan) following the manufacturer's instructions. The absorbance in each well was measured at a wavelength of 450 nm with a Multiskan FC plate reader (Thermo Fisher Scientific, Inc., USA). Each experiment was performed in triplicate. The cytotoxic effect of 5FU was assessed by the IC50 concept (34), and the IC50 value for 5FU was calculated using CompuSyn software (Chou and Martin, 2005, Compusyn, Inc., USA).

Statistical analysis. Statistical analyses were performed using Medcalc statistical software V.16.2.0 (Medcalc Software bvba, Ostend, Belgium), JMP software 10.0.2 (SAS Institute, Cary, NC, USA), and GraphPad Prism software ver.8.2.0 (GraphPad Software Inc., San Diego, CA). Comparison of IHC score between high- and low-expression groups and various clinicopathological factors in the clinical cohort were performed using Fisher's exact test. Comparisons of differential gene expression between two groups from *in vitro* experiments were performed using two-tailed unpaired Student's t-test. On the other hand, comparisons of differential gene expression between multiple groups from *in vitro* experiments were performed using one-way ANOVA with Tukey's multiple comparisons test. Comparisons of IHC scores between various stages were performed using Kruskal-Wallis test and Dunn's multiple comparisons test. Youden's index for dead/alive or recurrence/non-recurrence within the observation period was used to determine the optimal cutoff thresholds to dichotomize patients into high- and low-expression groups of GPX4 and HSPB1 using Medcalc statistical software. OS was defined as the period from the date of CRC diagnosis to the date of last known follow-up; recurrence-free survival (RFS) was defined as the period from the date of CRC diagnosis to the date of recurrence. Kaplan-Meier analyses for OS and RFS were performed by log-rank test. For OS and RFS survival analyses, we dichotomized patients into GPX4 or HSPB1 high- and low-expression groups as determined by receiver operating characteristic analysis (same as Youden's index) for dead/alive or recurrence/non-recurrence. Univariate and multivariate analyses for OS and RFS were performed using the Cox proportional hazards model to determine the factors affecting OS and RFS. $P<0.05$ was considered to indicate a statistically significant difference.

Results

Comprehensive in silico analysis identified GPX4 and HSPB1 as candidate prognostic biomarkers in colorectal cancer patients. As described in the Materials and Methods section, we determined SLC7A11, AIFM2, NFE2L2 (NRF2), FTH1, GLS2, GPX4, and HSPB1 genes as candidate negative regulators of ferroptosis. We then evaluated their prognostic importance by analyzing 367 CRC patients with available information on survival outcome in TCGA-COADREAD datasets. We dichotomized patients into high and low gene expression groups as determined by Youden's index for dead/alive. High expression of SLC7A11, AIFM2, NFE2L2, FTH1, and GLS2 genes did not stratify survival outcome of patients (Fig. 1B-F). In contrast, patients with high expression of GPX4 and HSPB1 genes showed significantly worse OS ($P<0.01$ for both factors) than those with low expression (Fig. 1G and H). Therefore, we selected GPX4 and HSPB1 as candidate targets for further validation study.

High GPX4 protein expression was associated with aggressive cancer phenotype in CRC patients. To evaluate the prognostic potential of GPX4 and HSPB1 in CRC patients, we first investigated GPX4 expression in a cohort of stage 1-4 CRC patients by IHC analysis. While GPX4 protein was not expressed or weakly expressed in the adjacent normal mucosa (Fig. 2A), it was expressed mainly in the cytoplasm of CRC cells (Fig. 2A). There was varying expression of GPX4 among CRC cases (Fig. 2B). The GPX4 IHC score for 151 CRC patients was 3.5±2.1 (mean ± SD), and median value for GPX4 IHC score was 4; 15 CRC patients with GPX4-negative staining were excluded from the analysis. The GPX4 IHC score of stage 1 CRC patients was significantly lower than those of stage

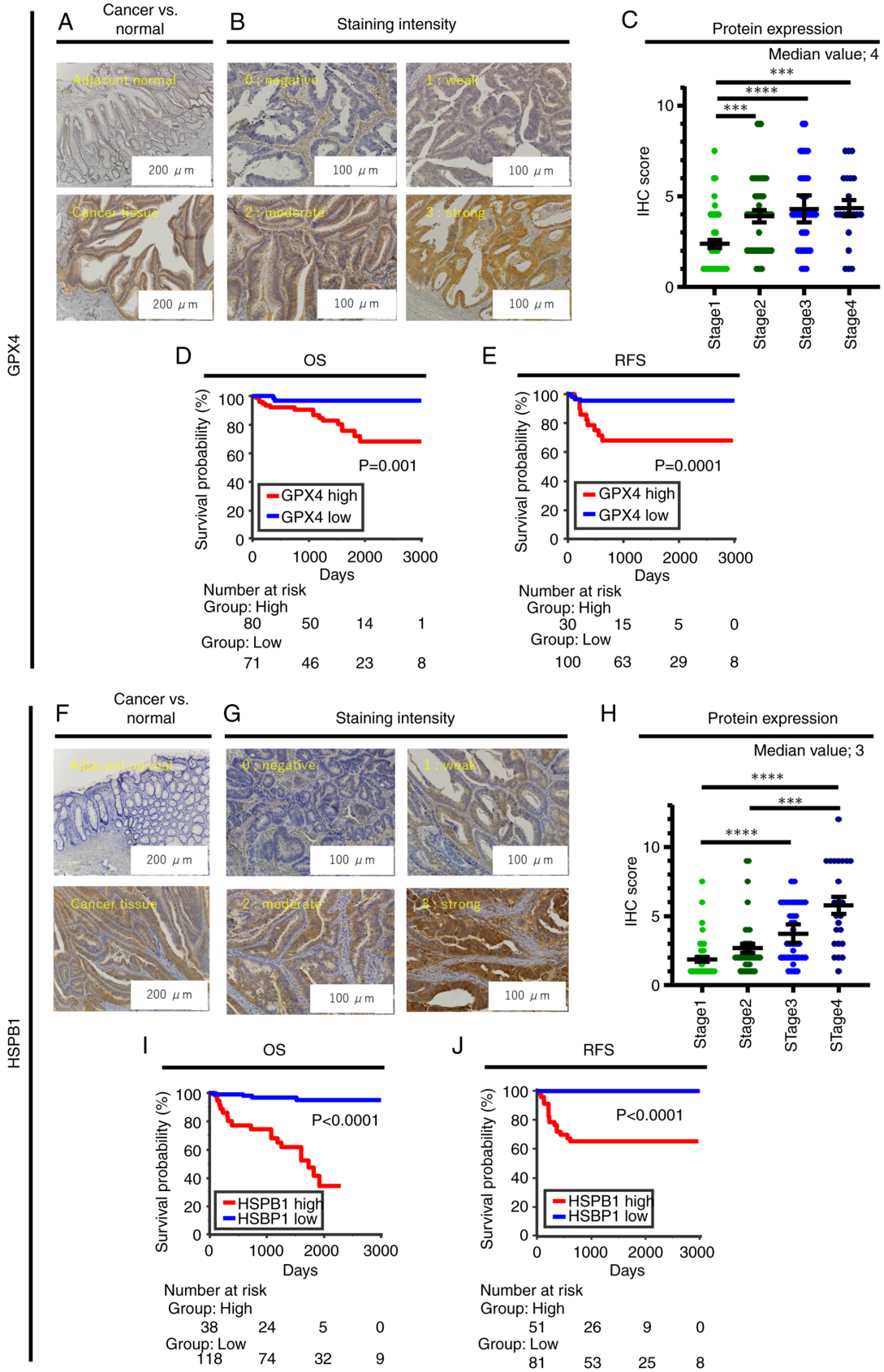

Figure 2. Representative images of immunohistochemistry of GPX4 and HSPB1 in CRC specimens and association between IHC score profiling, UICC stage, and survival outcome in CRC patients dichotomized by GPX4 and HSPB1 expression. (A) Representative image of GPX4 expression in adjacent colon normal mucosa and CRC tissue. (B) Representative staining intensity of GPX4 scored as 0 (negative), 1 (weak), 2 (moderate), and 3 (strong). (C) Dot plot showing the IHC score of GPX4 for stage 1 to stage 4 CRC patients. Kaplan-Meier analysis for (D) OS and (E) RFS in CRC patients classified into high/low GPX4 expression groups. (F) Representative image of HSPB1 expression in adjacent colon normal mucosa and CRC tissue. (G) Representative staining intensity of HSPB1 scored as 0 (negative), 1 (weak), 2 (moderate), and 3 (strong). (H) Dot plot showing the IHC score of HSPB1 for stage 1 to stage 4 CRC patients. Kaplan-Meier analysis for (I) OS and (J) RFS in CRC patients classified into high/low HSPB1 expression groups. ***P<0.001, and ****P<0.0001. CRC, colorectal cancer; OS, overall survival; RFS, recurrence-free survival; IHC, immunohistochemistry.

2-4 patients (Fig. 2C). We analyzed the association between GPX4 expression and clinicopathological parameters and found that high GPX4 expression (GPX4 IHC score ≥4) was significantly associated with larger tumor size (P=0.002), advanced T factor (P=0.003), lymph node metastasis positivity (P=0.002), lymphatic and venous invasion positivity (P=0.02 and P<0.001, respectively), and stage 4 cases (P=0.02) (Table I). These results indicate that high GPX4 protein expression was significantly associated with an aggressive cancer phenotype in CRC patients in the clinical cohort.

High GPX4 protein expression was associated with poor survival outcome in CRC patients. Next, we evaluated the prognostic value of GPX4 protein expression by examining OS using Kaplan-Meier analysis. Patients with high expression of GPX4 (GPX4 IHC score ≥4) exhibited significantly worse OS compared with patients with low expression (P=0.001, Fig. 2D). To elucidate whether GPX4 protein expression can be used for recurrence prediction, we investigated the association between GPX4 protein expression and postoperative recurrence by analyzing RFS of 130 stage 1-3 CRC patients receiving treatment with curative intent. In line with the OS data, patients with high expression of GPX4 (GPX4 IHC score ≥5; dichotomized by Youden's index for positive/negative recurrence) showed significantly worse RFS than those with low expression (P=0.0001, Fig. 2E).

To determine whether high GPX4 protein expression was a risk factor for OS or RFS, the Cox proportional hazard model was used to perform univariate and multivariate analysis. In univariate analysis for OS, along with high GPX4 protein expression (P=0.0005), several clinicopathological factors such as rectal cancer (P=0.02), invasive endoscopic type (P=0.04), larger tumor size (P=0.008), diffuse histological type (P=0.009), advanced T stage (P<0.0001), lymph node metastasis (P=0.0002), lymphatic and venous invasion positive cases (P=0.001 for both factors), and stage 4 cases (P<0.0001) were risk factors for poorer OS (Table II). Multivariate analysis showed that diffuse histological type [hazard ratio (HR)=6.48, P=0.02] and stage 4 cases (HR=5.61, P=0.009) were independent risk factors for poorer OS; high GPX4 expression did not show statistical significance (P=0.14, Table II).

With regard to univariate analysis for RFS, primary lesion in rectum (P=0.0007), invasive endoscopic type (P=0.049), advanced T stage and N stage (P=0.01, P=0.002, respectively), lymphatic and venous invasion positive cases (P=0.0007, P=0.002, respectively), and high GPX4 expression (P=0.018) were risk factors for poor RFS (Table II). Multivariate analysis showed that primary lesion in rectum (HR=6.83, P<0.0001), invasive endoscopic type (HR=5.91, P=0.008), lymphatic invasion positivity (HR=4.66, P=0.02), and high GPX4 expression (HR=4.11, P=0.03) were independent risk factors for poor RFS (Table II). Thus, high GPX4 expression may predict poor RFS in CRC patients.

High HSPB1 protein expression was associated with aggressive phenotype in CRC patients. We also investigated the prognostic potential of HSPB1 in the stage 1-4 CRC patients by IHC. While HSPB1 protein was absent or weakly expressed in the adjacent normal mucosa (Fig. 2F), it was expressed mainly in the cytoplasm of CRC cells (Fig. 2F), similar to the expression of GPX4. HSPB1 expression also varied among CRC cases (Fig. 2G). The HSPB1 IHC score for 156 patients was 3.1±2.4, and median value for HSPB1 IHC score was 3; 10 CRC patients with HSPB1-negative staining were eliminated from analysis. Notably, the IHC score trend of HSPB1 showed a more prominent 'stage-dependent elevated pattern' in CRC patients (Fig. 2H). Similar to the results with GPX4 expression, high HSPB1 expression (HSPB1 IHC score >4; dichotomized by Youden's index for OS) was significantly associated with aggressive cancer phenotypes such as diffuse histological type (P=0.03), advanced T factor (P=0.005), lymph node metastasis positivity (P<0.0001), lymphatic and venous invasion positivity (P<0.0001 for both factors), and stage 4 cases (P<0.0001) (Table I). Thus, similar to GPX4, high HSPB1 protein expression was significantly associated with aggressive cancer phenotype in CRC patients.

High HSPB1 protein expression showed strong robustness as a prognostic and recurrence-predictive biomarker in CRC patients. We further assessed the overall prognostic significance of HSPB1 protein expression by analyzing OS using the Kaplan-Meier method. Patients with high expression of HSPB1 (HSPB1 IHC score ≥5) showed significantly worse OS than patients with low expression (P<0.0001, Fig. 2I). Kaplan-Meier analysis for RFS in 132 stage 1-3 CRC patients treated with curative intent revealed that patients with high expression of HSPB1 (HSPB1 IHC score ≥3; dichotomized by Youden's index for positive/negative recurrence) showed significantly worse RFS than patients with low expression (P<0.0001, Fig. 2J).

We performed Cox proportional univariate and multivariate analysis for OS and RFS in the CRC patients. In univariate analysis for OS, along with high HSPB1 expression (P<0.0001), several aggressive phenotypes such as invasive endoscopic type (P=0.002), larger tumor size (P=0.002), diffuse histological type (P=0.002), advanced T stage and N stage (P<0.0001 for both factors), lymphatic and venous invasion positive cases (P=0.002, P=0.001, respectively), and stage 4 cases (P<0.0001) were risk factors for poor OS (Table III). Multivariate analysis identified that diffuse histological type (HR=5.84, P=0.01), stage 4 patients (HR=3.99, P=0.02), and high HSPB1 expression (HR=6.35, P=0.006) were independent risk factors for poor OS (Table III). Regarding univariate analysis for RFS, primary lesion in rectum (P=0.0007), invasive endoscopic type (P=0.049), advanced T stage and N stage (P=0.01, P=0.002, respectively), lymphatic and venous invasion positivity (P=0.0007, P=0.002, respectively), and high HSPB1 expression (P<0.0001) were risk factors for poor RFS (Table III). Multivariate analysis demonstrated that primary lesion in rectum (P=0.0003), advanced T stage (P=0.009), and high HSPB1 expression (P<0.0001) were independent risk factors for poor RFS (Table III). These results indicate that high HSPB1 expression may indicate poor prognosis and high risk of recurrence in CRC patients, and its biomarker potential may be superior to that of GPX4.

GPX4 and HSPB1 may be biomarkers in advanced CRC patients treated with adjuvant therapy with curative intent. We next investigated whether GPX4 and HSPB1 expressions were biomarkers for adjuvant chemotherapy in advanced (stage

Table I. Association between clinicopathological factors and expression of GPX4 and HSPB1 in the in-house clinical cohort.

	GPX4				HSPB1			
Variable	Number	Low (n=71)	High (n=80)	P-value	Number	Low (n=118)	High (n=38)	P-value
Age at operation, years								
>69	86	39	47		88	70	18	
<69	65	32	33	0.74	68	48	20	0.26
Sex								
Male	86	39	47		85	67	18	
Female	65	32	33	0.74	71	51	20	0.35
Tumor location								
Colon	98	49	49		101	81	20	
Rectum	53	22	31	0.39	55	37	18	0.08
Macroscopic type								
Type 1, 2	137	68	69		138	107	31	
Type 3, 4	14	3	11	0.06	18	11	7	0.15
Tumor size, mm								
>40	102	57	45		51	35	16	
<40	49	14	35	0.002[a]	105	83	22	0.17
Histological type								
Intestinal	140	67	73		145	113	32	
Diffuse	11	4	7	0.54	11	5	6	0.03[a]
T factor								
T1, T2, T3	128	67	61		131	105	26	
T4	23	4	19	0.003[a]	25	13	12	0.005[a]
Lymph node metastasis								
Negative	97	55	42		97	89	8	
Positive	54	16	38	0.002[a]	59	29	30	<0.0001[a]
Lymphatic invasion								
Negative	65	38	27		65	60	5	
Positive	86	33	53	0.02[a]	91	58	33	<0.0001[a]
Venous invasion								
Negative	73	45	28		74	67	7	
Positive	78	26	52	0.0006[a]	82	51	31	<0.0001[a]
UICC stage								
1, 2, 3	130	66	64		132	109	23	
4	21	5	16	0.02[a]	24	9	15	<0.0001[a]

[a]P<0.05. Age and tumor size were dichotomized by median value. GPX4 and HSPB1 were dichotomized by Youden index for overall survival.

2 and 3) CRC patients. We first investigated the association between clinicopathological factors and GPX4 and HSPB1 expressions by Fisher's exact test. We dichotomized cases into high- and low-expression groups by Youden index for RFS. While there was no significant correlation between the clinicopathological factors and GPX4 expression, the frequency of patients with high expression of HSPB1 was significantly higher in cases with rectal cancer and cases with positive lymph node metastasis (Table SII).

We then evaluated the recurrence prediction potential of GPX4 and HSPB1 by Kaplan-Meier analysis in stage 2 CRC patients who were not administered adjuvant chemotherapy. While there was no significant difference in RFS between patients with high and low GPX4 expression (P=0.18), the recurrence rate of patients with high GPX4 expression was worse than those with low expression (HR=4.52) (Fig. S1A). Patients with HSPB1 high expression showed significantly worse RFS than those with low expression (P=0.0002). HR could not be calculated because no patients with HSPB1 low expression showed recurrence (Fig. S1B).

We next evaluated RFS in stage 2 and 3 CRC patients who were treated with capecitabine. While there was no significant difference for RFS between patients with high and low GPX4 expression (P=0.26), the recurrence rate of patients with high

Table II. Multivariate analysis for overall survival and recurrence-free survival and GPX4 expression in clinical cohort.

A, Overall survival (n=151)

	Univariate analysis			Multivariate analysis		
Variable	HR	95%CI	P-value	HR	95%CI	P-value
Age >70 years	0.95	0.37-2.44	0.92			
Male	1.9	0.72-5.92	0.2			
Tumor location rectum	3.07	1.21-8.36	0.02[a]	2.41	0.83-7.47	0.11
Macroscopic type 3/4/5	3.75	1.06-10.50	0.04[a]	3.02	0.65-13.20	0.15
Tumor size >40 mm	3.53	1.39-9.60	0.008[a]	0.67	0.20-2.31	0.52
Poorly differentiated histology	5.98	1.68-16.95	0.009[a]	6.48	1.30-28.66	0.02[a]
T stage greater than T4	11.74	4.59-32.12	<0.0001[a]	2.31	0.61-8.92	0.22
Lymph node metastasis positive	6.39	2.29-22.57	0.0002[a]	1.64	0.44-7.98	0.48
Lymphatic invasion positive	6.76	1.92-42.77	0.001[a]	2.29	0.38-19.39	0.38
Venous invasion positive	7.04	2.00-44.53	0.001[a]	1.79	0.38-13.10	0.48
Metastasis positive	20.55	7.91-59.41	<0.0001[a]	5.61	1.55-20.82	0.009[a]
GPX4 protein high	7.92	2.25-50.12	0.0005[a]	3.29	0.70-24.64	0.14

B, Recurrence-free survival (n=130)

	Univariate analysis			Multivariate analysis		
Variable	HR	95%CI	P-value	HR	95%CI	P-value
Age >70 years	0.99	0.33-3.10	0.99			
Male	1.1	0.37-3.65	0.86			
Tumor location rectum	7.02	2.15-31.34	0.0009[a]	7.07	2.12-32.02	0.001[a]
Macroscopic type 3/4/5	1.32	0.07-6.70	0.8			
Tumor size >40 mm	1.05	0.28-3.21	0.94			
Poorly differentiated histology	5.13E-09	2.78-2.78	0.23			
T Stage greater than T4	1.88	0.29-7.01	0.45			
Lymph node metastasis positive	3.77	1.26-12.48	0.02[a]	1.56	0.48-5.72	0.46
Lymphatic invasion positive	13.4	2.64-243.96	0.0005[a]	7.71	1.27-150.89	0.02[a]
Venous invasion positive	6.53	1.75-42.20	0.004[a]	1.35	0.23-11.06	0.75
GPX4 protein high	7.68	2.50-28.35	0.0004[a]	4.11	1.18-17.83	0.03[a]

[a]P<0.05. Age and tumor size were dichotomized by median value. GPX4 was dichotomized by Youden index for overall survival and recurrence-free survival. HR, hazard ratio; CI, confidence interval.

expression of GPX4 was worse than that of patients with low expression (HR=3.61, Fig. S2A). Similarly, for HSPB1, while there was no significant difference of RFS between high- and low-expression groups (P=0.25), patients with high expression of HSPB1 showed worse recurrence rates than those with low expression (HR=3.52, Fig. S2B).

Collectively, our findings showed that HSPB1 expression indicated recurrence in stage 2 and 3 CRC patients treated with curative intent. In patients with high expression of HSPB1, we may recommend administration or reinforcement of adjuvant chemotherapy. However, further studies with more patients are required to strengthen our findings.

GPX4 and HSPB1 may be associated with 5-fluorouracil resistance in CRC cells in vitro. On the basis of the results of subgroup analysis for GPX4 and HSPB1 in advanced CRC patients treated with adjuvant therapy with curative intent, we further investigated the functional role of GPX4 and HSPB1 in the response to 5-fluorouracil (5FU)-based chemotherapy using CRC cell lines. First, we evaluated the mRNA and protein expression of GPX4 and HSPB1 in four CRC cell lines (DLD-1, RKO, SW480, and LOVO) (Fig. 3A and B). We selected DLD-1 and SW480 for further experiments, as both GPX4 and HSPB1 mRNA and protein were detected at higher levels in these two cell lines. Next, we transfected GPX4 and HSPB1 siRNA in these two CRC cell lines and confirmed effective knockdown of mRNA (Fig. 3C) and protein levels (Fig. 3D) of both factors. We then compared the cytotoxic effect of 5FU between cells transfected with negative control siRNA and cells transfected with siRNA against GPX4 and

Table III. Multivariate analysis for overall survival and recurrence-free survival and HSPB1 expression in clinical cohort.

A, Overall survival (n=156)

	Univariate analysis			Multivariate analysis		
Variable	HR	95%CI	P-value	HR	95%CI	P-value
Age >70 years	0.94	0.40-2.21	0.89			
Male	1.33	0.57-3.34	0.51			
Tumor location rectum	2.28	0.98-5.41	0.06			
Macroscopic type 3/4/5	4.92	1.88-11.69	0.002[a]	3.19	0.99-10.26	0.06
Tumor size >40 mm	3.96	1.69-9.91	0.002[a]	1.04	0.32-3.25	0.95
Poorly differentiated histology	6.61	2.15-16.96	0.002[a]	5.84	1.56-20.05	0.01[a]
T stage greater than T4	10.64	4.56-25.96	<0.0001[a]	1.79	0.46-6.83	0.4
Lymph node metastasis positive	10.87	3.70-46.29	<0.0001[a]	2.1	0.55-11.37	0.3
Lymphatic invasion positive	5.21	1.78-22.19	0.002[a]	1.28	0.33-6.70	0.74
Venous invasion positive	5.41	1.84-23.04	0.001[a]	0.95	0.23-5.00	0.95
Metastasis positive	15.31	6.51-38.55	<0.0001[a]	3.99	1.23-13.40	0.02[a]
HSPB1 protein high	16.69	6.20-57.96	<0.0001[a]	6.35	1.67-31.59	0.006[a]

B, Recurrence-free survival (n=132)

	Univariate analysis			Multivariate analysis		
Variable	HR	95%CI	P-value	HR	95%CI	P-value
Age >70 years	1.09	0.40-30.8	0.87			
Male	0.96	0.36-2.68	0.93			
Tumor location rectum	4.82	1.75-15.31	0.002[a]	5.96	1.83-22.97	0.003[a]
Macroscopic type 3/4/5	3.67	1.03-10.56	0.047[a]	1.85	0.42-7.28	0.39
Tumor size >40 mm	1.83	0.65-4.91	0.24			
Poorly differentiated histology	1.31	0.07-6.48	0.8			
T stage greater than T4	3.58	1.00-10.30	0.05[a]	6.02	1.20-28.53	0.03[a]
Lymph node metastasis positive	3.9	1.45-11.45	0.007[a]	0.9	0.24-3.80	0.88
Lymphatic invasion positive	15.73	3.19-284.38	<0.001[a]	11.87	1.45-276.49	0.02[a]
Venous invasion positive	8.05	2.5-51.28	0.0006[a]	0.9	0.15-7.49	0.91
HSPB1 protein high	1.01E+10	14.76-14.76	<0.001[a]	8.57E+09	12.06-1.05e+55	<0.001[a]

[a]P<0.05. Age and tumor size were dichotomized by median value. HR; hazard ratio, CI; confidence interval. HSPB1 was dichotomized by Youden index for overall survival and recurrence-free survival.

HSPB1 using WST8 assays. The IC50 values of 5FU were decreased in cells transfected with GPX4 siRNA (DLD-1, from 106.03 to 58.13 μM; SW480, 67.61 to 24.73 μM) and HSPB1 siRNA (DLD-1, from 106.03 to 67.62 μM; SW480, 67.61 to 18.93 μM) (Fig. 3E). Collectively, these *in vitro* experiments demonstrated that GPX4 and HSPB1 may play crucial roles in attenuating the cytotoxic effect of 5FU-based conventional chemotherapy.

Discussion

Accumulating evidence has revealed the association between ferroptosis regulators and cancer development in CRC (35,36). In this study, we performed comprehensive *in silico* dataset analysis and evaluated the association between the expression of negative regulators of ferroptosis and CRC prognosis; we also performed validation in clinical specimens from CRC patients by IHC. Our findings indicate that high expressions of HSPB1 and GPX4 may serve as prognostic biomarkers for poor outcomes in CRC patients.

Ferroptosis is a newly defined iron-dependent non-apoptotic cell death form characterized by lipid peroxidation, iron accumulation, and accumulation of lipid ROS (12). Ferroptosis is distinguished from other regulated cell death by differences in morphology, genetics, and biochemistry (12). Multiple studies have shown that ferroptosis is involved in multiple pathological processes including tumorigenesis and cancer development (15-17). Several studies have shown that the initiation of ferroptosis in CRC cells successfully eliminates cancer cells that are resistant to other forms of regulated cell

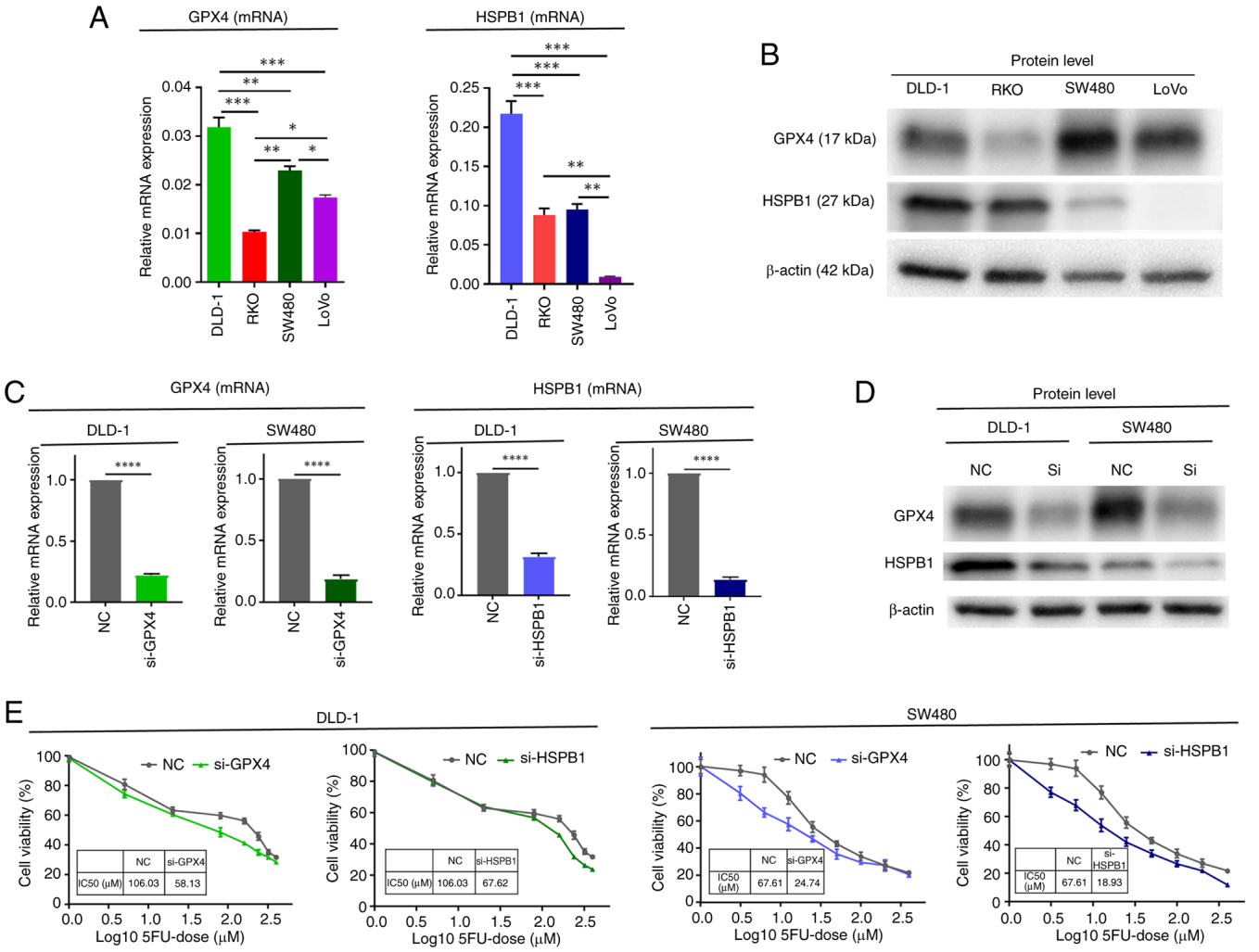

Figure 3. Evaluation of the cytotoxic effect of 5-fluorouracil-based chemotherapy in CRC cell lines after transfection of GPX4 and HSPB1 siRNA. (A) mRNA expression of GPX4 and HSPB1 in four CRC cell lines. (B) Western blotting image of GPX4 and HSPB1 in four CRC cell lines. (C) GPX4 and HSPB1 mRNA levels in DLD1/SW480 cell lines after transfection of GPX4 and HSPB1 siRNA. (D) GPX4 and HSPB1 protein levels in DLD1/SW480 cell lines after transfection of GPX4 and HSPB1 siRNA. (E) Cytotoxic effect of 5-fluorouracil-based chemotherapy in DLD1 and SW480 cell lines after transfection of GPX4 and HSPB1 siRNA. *P<0.05, **P<0.01, ***P<0.001, and ****P<0.0001. CRC, colorectal cancer; NC, negative control; 5FU, 5-fluorouracil; siRNA, small interfering RNA.

death (35,36). Moreover, GSH, RSL3, ACSL4, LCN2, SRSF9, GCH1, TMEM16F, SLC7A11, NRF2, and p53 may play a pivotal role in CRC by ferroptosis-related pathways (37-51). Hence, we hypothesized that negative regulators of ferroptosis may also have an important role in CRC progression. In this study, we performed a comprehensive analysis of public datasets to explore candidate negative regulators of ferroptosis in CRC.

After the publication of TCGA project of multiple malignancies including alimentary tract cancer (52-54), comprehensive expression profiling information is more easily available and biomarker studies using bioinformatic analysis are ongoing each year. One bioinformatic study examined the relationship between ferroptosis-associated gene expression and prognosis of CRC patients to establish a predictive model and explored the potential value of ferroptosis as a therapeutic target (55). Shao *et al* identified ferroptosis-related differentially expressed genes between tumor and normal colon tissues from the GeneCards and FerrDb websites and analyzed the prognostic information of CRC patients from TCGA dataset and other public datasets (55). The authors identified a 10-gene prognostic signature consisting of TFAP2C, SLC39A8, NOS2, HAMP, GDF15, FDFT1, CDKN2A, ALOX12, AKR1C1, and ATP6V1G2 genes; they demonstrated that the signature score could effectively predict the prognosis of CRC patients and the signature score of cetuximab-resistant CRC patients was significantly higher than that of sensitive patients (55). Although the study indicated the importance of this 10-gene signature, their in-house investigation included a small amount of evidence such as tissue microarray of FDFT1, GDF15, HAMP, and TFAP2C to evaluate their differential expression in 75-paired normal/tumor CRC specimens (55). In our study, we examined negative regulators of ferroptosis in cancer progression and demonstrated that HSPB1 and GPX4 were prognostic biomarkers of CRC patients.

Heat shock proteins increase the migration ability, decrease apoptosis, and are involved in chemoresistance in cancer cells (56,57). HSPB1, a chaperone protein also known as heat shock 27kD protein 1 (HSP27), is stimulated by transcriptional factor heat shock factor-1 (HSF-1) after elastin treatment

and stabilizes proteins under stress (58). Phosphorylation of HSPB1 by protein kinase C regulates iron uptake, reduces iron-mediated production of ROS and inhibits elastin-induced ferroptosis (58). Inhibition of the HSF1-HSPB1 pathway increased the elastin-mediated anticancer activity in human cervical carcinoma xenograft mouse models, and an essential role for HSPB1 on ferroptosis-mediated cancer therapy was indicated (58).

HSPB1 has also been reported to influence both cancer progression and chemoresistance (59,60). Several studies have shown that upregulation of HSPB1 induces chemoresistance or resistance to radiotherapy in lung (61), breast (62), and colon cancers (63,64). Several studies showed that HSPB1 suppression increased the sensitivity of colon cancer cells to 5FU (63,65) and irinotecan (66). Furthermore, Liu *et al* conducted *in vitro* and *in vivo* studies and found that suppression of HSPB1 induced inhibition of tumor progression and enhancement of sensitivity to 5FU and vincristine via suppression of the NOTCH1/Akt/mTOR signaling pathway in colon cancer cells (67). Thus, HSPB1 may be a promising target with a critical role in CRC development and drug resistance. Further studies on the mechanism of HSPB1 as a negative regulator of ferroptosis in CRC should be performed.

GPX4 converts reduced GSH to oxidized glutathione and reduces lipid hydroperoxides. The function of GPX4 is mainly inhibited by Ras-selective lethal small molecule 3 (RSL3) or ferroptosis-inducing agents such as DPI7 (68-70). Knockdown of GPX4 induces ferroptosis in a MAPK/ERK kinase-, iron-, and ROS-dependent manner (69). Zhang *et al* established 5FU- and AZ628-resistant CRC cells, revealed the characteristics of the resistant cell lines by *in vitro* assays, and evaluated the efficacy and mechanism of GPX4 inhibitor by *in vitro* and *in vivo* experiments (71). While resistant cell lines exhibited drug sensitivity, GPX4 expression was significantly upregulated in resistant cells, and persister cells were more sensitive and underwent ferroptosis induced by the GPX4 inhibitor. Studies in a mouse model revealed that GPX4 inhibition restrained tumor regrowth after discontinuation of anti-CRC drug treatment (71). The authors concluded that upregulated GPX4 in drug-resistant cells was a potential therapeutic target and GPX4 inhibition by combination chemotherapy with molecular targeted therapy may be a promising anti-CRC treatment (71). From this evidence, GPX4 may be a therapeutic target for CRC development and chemoresistance. The mechanisms and downstream targets of GPX4 should be explored in future studies.

In this study, subgroup analysis of stage 2-3 CRC patients showed that HSPB1 expression could clearly stratify the recurrence prognosis of this patient group. We recommend administration or reinforcement of adjuvant chemotherapy in patients with high expression of HSPB1. While National Comprehensive Cancer Network and Japanese Society for Cancer of the Colon and Rectum have provided definitions for high-risk stage 2 CRC patients (72,73), there are still controversial issues regarding the detailed regimen or administration period of adjuvant chemotherapy. A recent prospective randomized phase III ACHIEVE-2 trial revealed that three months of adjuvant chemotherapy of mFOLFOX6/CAPOX showed significantly less adverse effects and 3-year RFS did not differ compared with the six-month regimen in high-risk stage 2 colon cancer patients (74). In future studies, we will analyze a larger group of patients and investigate whether HSPB1 may be a biomarker to help provide detailed directions for adjuvant chemotherapy treatment.

This study has several limitations. First, this was a retrospective single institutional study with a relatively small sample size. There were some patients (approximately 6.6%, data not shown) whose postoperative follow-up period was short (less than 30 days) because of lost follow-up. Additionally, while we found that GPX4 and HSPB1 may exhibit important roles in attenuating the cytotoxic effect of conventional cytotoxic chemotherapy through *in vitro* experiments, we could not directly confirm induction of ferroptosis in response to siRNA transfection of GPX4 or HSPB1 because of technical limitations. Therefore, in the future, multi-center large sample number studies are warranted and in-depth mechanistic experiments are required to reveal the detailed biological function of GPX4 and HSPB1, especially in the negative regulation of ferroptosis in CRC.

In conclusion, our study provides novel insights into the prognostic biomarker potential of negative regulators of ferroptosis in CRC patients using *in silico* identification and evaluation and validation in clinical samples. Moreover, attenuation of the cytotoxic effect of chemotherapy induced by GPX4 and HSPB1 may be one of the mechanisms to shorten the overall and/or recurrence-free prognosis of CRC patients with high GPX4 and HSPB1 expression. Collectively, our results demonstrated that GPX4 and HSPB1 may be effective biomarkers to predict the survival outcome and postoperative recurrence in CRC patients.

Acknowledgements

The authors would like to acknowledge Ms. Yuki Orito and Ms. Amphone Okada (Department of Gastrointestinal and Pediatric Surgery, Mie University Graduate School of Medicine) for experimental support, and Dr Gabrielle White Wolf for editing a draft of this manuscript.

Funding

This work was partially supported by a Grant in Aid for Scientific Research (grant nos. 22K08868 and 23K08210) from the Ministry of Education, Culture, Sports, Science, and Technology, Japan.

Availability of data and materials

The data generated in the present study may be requested from the corresponding author.

Authors' contributions

TS, CY, YOku and YT contributed to conceptualization and design of the study. TS, CY, RM, AZ, YN, AS, HO, XZ, YOku and YT acquired, analyzed or interpretated the data. TS, CY, YOku and YT drafted the manuscript. TS, CY, RM, AZ, SYa, KH, YS, HImao, TK, MK, YK, YOki, SYo, MO, AH, HImai, YOku and YT performed statistical analysis. CY, RM, AZ, YN, AS, HO, AH, HImai and YOku provided administrative,

technical or material support. YT supervised the study. TS and CY confirm the authenticity of all the raw data. All authors read and approved the final version of the manuscript.

Ethics approval and consent to participate

All study-related procedures were performed as per The Declaration of Helsinki, wherein a written informed consent was obtained from each patient, and the Institutional Review Board (IRB) of Medical Ethics Committee of Mie University Graduate School of Medicine approved this study (IRB number: H2023-172).

Patient consent for publication

Not applicable.

Competing interests

The authors declare that they have no competing interests.

References

1. Siegel RL, Miller KD, Fedewa SA, Ahnen DJ, Meester RGS, Barzi A and Jemal A: Colorectal cancer statistics, 2017. CA Cancer J Clin 67: 177-193, 2017.
2. Gill S, Loprinzi CL, Sargent DJ, Thomé SD, Alberts SR, Haller DG, Benedetti J, Francini G, Shepherd LE, Francois Seitz J, *et al*: Pooled analysis of fluorouracil-based adjuvant therapy for stage II and III colon cancer: Who benefits and by how much? J Clin Oncol 22: 1797-1806, 2004.
3. Meyerhardt JA: Adjuvant therapy for stage II and III colon cancer. Clin Adv Hematol Oncol 8: 772-774, 2010.
4. Wu C: Systemic therapy for colon cancer. Surg Oncol Clin N Am 27: 235-242, 2018.
5. Dallas NA, Xia L, Fan F, Gray MJ, Gaur P, van Buren G II, Samuel S, Kim MP, Lim SJ and Ellis LM: Chemoresistant colorectal cancer cells, the cancer stem cell phenotype, and increased sensitivity to insulin-like growth factor-I receptor inhibition. Cancer Res 69: 1951-1957, 2009.
6. Hu T, Li Z, Gao CY and Cho CH: Mechanisms of drug resistance in colon cancer and its therapeutic strategies. World J Gastroenterol 22: 6876-6889, 2016.
7. Holohan C, Van Schaeybroeck S, Longley DB and Johnston PG: Cancer drug resistance: An evolving paradigm. Nat Rev Cancer 13: 714-726, 2013.
8. Ganesh K, Stadler ZK, Cercek A, Mendelsohn RB, Shia J, Segal NH and Diaz LA Jr: Immunotherapy in colorectal cancer: Rationale, challenges and potential. Nat Rev Gastroenterol Hepatol 16: 361-375, 2019.
9. Li J, Guo BC, Sun LR, Wang JW, Fu XH, Zhang SZ, Poston G and Ding KF: TNM staging of colorectal cancer should be reconsidered by T stage weighting. World J Gastroenterol 20: 5104-5112, 2014.
10. Gallois C, Pernot S, Zaanan A and Taieb J: Colorectal cancer: Why does side matter? Drugs 78: 789-798, 2018.
11. Duffy MJ: Carcinoembryonic antigen as a marker for colorectal cancer: Is it clinically useful? Clin Chem 47: 624-630, 2001.
12. Dixon SJ, Lemberg KM, Lamprecht MR, Skouta R, Zaitsev EM, Gleason CE, Patel DN, Bauer AJ, Cantley AM, Yang WS, *et al*: Ferroptosis: an iron-dependent form of nonapoptotic cell death. Cell 149: 1060-1072, 2012.
13. Wang Y, Wei Z, Pan K, Li J and Chen Q: The function and mechanism of ferroptosis in cancer. Apoptosis 25: 786-798, 2020.
14. Hassannia B, Vandenabeele P and Vanden Berghe T: Targeting ferroptosis to iron out cancer. Cancer Cell 35: 830-849, 2019.
15. Friedmann Angeli JP, Schneider M, Proneth B, Tyurina YY, Tyurin VA, Hammond VJ, Herbach N, Aichler M, Walch A, Eggenhofer E, *et al*: Inactivation of the ferroptosis regulator Gpx4 triggers acute renal failure in mice. Nat Cell Biol 16: 1180-1191, 2014.
16. Matsushita M, Freigang S, Schneider C, Conrad M, Bornkamm GW and Kopf M: T cell lipid peroxidation induces ferroptosis and prevents immunity to infection. J Exp Med 212: 555-568, 2015.
17. Chen L, Hambright WS, Na R and Ran Q: Ablation of the ferroptosis inhibitor glutathione peroxidase 4 in neurons results in rapid motor neuron degeneration and paralysis. J Biol Chem 290: 28097-28106, 2015.
18. Shi ZZ, Fan ZW, Chen YX, Xie XF, Jiang W, Wang WJ, Qiu YT and Bai J: Ferroptosis in carcinoma: Regulatory mechanisms and new method for cancer therapy. Onco Targets Ther 12: 11291-11304, 2019.
19. Chen P, Li X, Zhang R, Liu S, Xiang Y, Zhang M, Chen X, Pan T, Yan L, Feng J, *et al*: Combinative treatment of β-elemene and cetuximab is sensitive to KRAS mutant colorectal cancer cells by inducing ferroptosis and inhibiting epithelial-mesenchymal transformation. Theranostics 10: 5107-5119, 2020.
20. Sharma P, Shimura T, Banwait JK and Goel A: Andrographis-mediated chemosensitization through activation of ferroptosis and suppression of β-catenin/Wnt-signaling pathways in colorectal cancer. Carcinogenesis 41: 1385-1394, 2020.
21. Shimura T, Sharma P, Sharma GG, Banwait JK and Goel A: Enhanced anti-cancer activity of andrographis with oligomeric proanthocyanidins through activation of metabolic and ferroptosis pathways in colorectal cancer. Sci Rep 11: 7548, 2021.
22. Ma R, Shimura T, Yin C, Okugawa Y, Kitajima T, Koike Y, Okita Y, Ohi M, Uchida K, Goel A, *et al*: Antitumor effects of andrographis via ferroptosis-associated genes in gastric cancer. Oncol Lett 22: 523, 2021.
23. Xie Y, Hou W, Song X, Yu Y, Huang J, Sun X, Kang R and Tang D: Ferroptosis: Process and function. Cell Death Differ 23: 369-379, 2016.
24. Edge SB and Compton CC: The American joint committee on cancer: The 7th edition of the AJCC cancer staging manual and the future of TNM. Ann Surg Oncol 17: 1471-1474, 2010.
25. Sharma A and Flora SJS: Positive and negative regulation of ferroptosis and its role in maintaining metabolic and redox homeostasis. Oxid Med Cell Longev 2021: 9074206, 2021.
26. Chen X, Li J, Kang R, Klionsky DJ and Tang D: Ferroptosis: Machinery and regulation. Autophagy 17: 2054-2081, 2021.
27. Ouyang S, Li H, Lou L, Huang Q, Zhang Z, Mo J, Li M, Lu J, Zhu K, Chu Y, *et al*: Inhibition of STAT3-ferroptosis negative regulatory axis suppresses tumor growth and alleviates chemoresistance in gastric cancer. Redox Biol 52: 102317, 2022.
28. Hu W, Zhang C, Wu R, Sun Y, Levine A and Feng Z: Glutaminase 2, a novel p53 target gene regulating energy metabolism and antioxidant function. Proc Natl Acad Sci USA 107: 7455-7460, 2010.
29. Wu S, Li T, Liu W and Huang Y: Ferroptosis and cancer: Complex relationship and potential application of exosomes. Front Cell Dev Biol 9: 733751, 2021.
30. Shimura T, Toiyama Y, Tanaka K, Saigusa S, Kitajima T, Kondo S, Okigami M, Yasuda H, Ohi M, Araki T, *et al*: Angiopoietin-like protein 2 as a predictor of early recurrence in patients after curative surgery for gastric cancer. Anticancer Res 35: 4633-4639, 2015.
31. Ichikawa T, Okugawa Y, Toiyama Y, Tanaka K, Yin C, Kitajima T, Kondo S, Shimura T, Ohi M, Araki T and Kusunoki M: Clinical significance and biological role of L1 cell adhesion molecule in gastric cancer. Br J Cancer 121: 1058-1068, 2019.
32. Mori K, Toiyama Y, Otake K, Ide S, Imaoka H, Okigami M, Okugawa Y, Fujikawa H, Saigusa S, Hiro J, *et al*: Successful identification of a predictive biomarker for lymph node metastasis in colorectal cancer using a proteomic approach. Oncotarget 8: 106935-106947, 2017.
33. Shigemori T, Toiyama Y, Okugawa Y, Yamamoto A, Yin C, Narumi A, Ichikawa T, Ide S, Shimura T, Fujikawa H, *et al*: Soluble PD-L1 expression in circulation as a predictive marker for recurrence and prognosis in gastric cancer: Direct comparison of the clinical burde between tissue and serum PD-L1 expression. Ann Surg Oncol 26: 876-883, 2019.
34. Stewart MJ and Watson ID: Standard units for expressing drug concentrations in biological fluids. Br J Clin Pharmacol 16: 3-7, 1983.
35. Wang Y, Zhang Z, Sun W, Zhang J, Xu Q, Zhou X and Mao L: Ferroptosis in colorectal cancer: Potential mechanisms and effective therapeutic targets. Biomed Pharmacother 153: 113524, 2022.
36. Liang X, You Z, Chen X and Li J: Targeting ferroptosis in colorectal cancer. Metabolites 12: 745, 2022.

37. Chen HHW and Kuo MT: Role of glutathione in the regulation of Cisplatin resistance in cancer chemotherapy. Met Based Drugs 2010: 430939, 2010.
38. Sui X, Zhang R, Liu S, Duan T, Zhai L, Zhang M, Han X, Xiang Y, Huang X, Lin H and Xie T: RSL3 drives ferroptosis through GPX4 inactivation and ROS production in colorectal cancer. Front Pharmacol 9: 1371, 2018.
39. Wang W, Green M, Choi JE, Gijón M, Kennedy PD, Johnson JK, Liao P, Lang X, Kryczek I, Sell A, *et al*: $CD8^+$ T cells regulate tumour ferroptosis during cancer immunotherapy. Nature 569: 270-274, 2019.
40. Tian X, Li S and Ge G: Apatinib promotes ferroptosis in colorectal cancer cells by targeting ELOVL6/ACSL4 signaling. Cancer Manag Res 13: 1333-1342, 2021.
41. Chaudhary N, Choudhary BS, Shah SG, Khapare N, Dwivedi N, Gaikwad A, Joshi N, Raichanna J, Basu S, Gurjar M, *et al*: Lipocalin 2 expression promotes tumor progression and therapy resistance by inhibiting ferroptosis in colorectal cancer. Int J Cancer 149: 1495-1511, 2021.
42. Wang R, Su Q, Yin H, Wu D, Lv C and Yan Z: Inhibition of SRSF9 enhances the sensitivity of colorectal cancer to erastin-induced ferroptosis by reducing glutathione peroxidase 4 expression. Int J Biochem Cell Biol 134: 105948, 2021.
43. Xiang R, Fu J, Ge Y, Ren J, Song W and Fu T: Identification of subtypes and a prognostic gene signature in colon cancer using cell differentiation trajectories. Front Cell Dev Biol 9: 705537, 2021.
44. Ousingsawat J, Schreiber R and Kunzelmann K: TMEM16F/anoctamin 6 in ferroptotic cell death. Cancers (Basel) 11: 625, 2019.
45. Guo C, Liu P, Deng G, Han Y, Chen Y, Cai C, Shen H, Deng G and Zeng S: Honokiol induces ferroptosis in colon cancer cells by regulating GPX4 activity. Am J Cancer Res 11: 3039-3054, 2021.
46. Chen Y, Zhang F, Du Z, Xie J, Xia L, Hou X, Hao E and Deng J: Proteome analysis of Camellia nitidissima Chi revealed its role in colon cancer through the apoptosis and ferroptosis pathway. Front Oncol 11: 727130, 2021.
47. He J, Ding H, Li H, Pan Z and Chen Q: Intra-tumoral expression of SLC7A11 is associated with immune microenvironment, drug resistance, and prognosis in cancers: A pan-cancer analysis. Front Genet 12: 770857, 2021.
48. Gnanapradeepan K, Basu S, Barnoud T, Budina-Kolomets A, Kung CP and Murphy ME: The p53 tumor suppressor in the control of metabolism and ferroptosis. Front Endocrinol (Lausanne) 9: 124, 2018.
49. Wei G, Sun J, Hou Z, Luan W, Wang S, Cui S, Cheng M and Liu Y: Novel antitumor compound optimized from natural saponin Albiziabioside A induced caspase-dependent apoptosis and ferroptosis as a p53 activator through the mitochondrial pathway. Eur J Med Chem 157: 759-772, 2018.
50. Wei R, Zhao Y, Wang J, Yang X, Li S, Wang Y, Yang X, Fei J, Hao X, Zhao Y, *et al*: Tagitinin C induces ferroptosis through PERK-Nrf2-HO-1 signaling pathway in colorectal cancer cells. Int J Biol Sci 17: 2703-2717, 2021.
51. Yang L, WenTao T, ZhiYuan Z, Qi L, YuXiang L, Peng Z, Ke L, XiaoNa J, YuZhi P, MeiLing J, *et al*: Cullin-9/p53 mediates HNRNPC degradation to inhibit erastin-induced ferroptosis and is blocked by MDM2 inhibition in colorectal cancer. Oncogene 41: 3210-3221, 2022.
52. Cancer Genome Atlas Network: Comprehensive molecular characterization of human colon and rectal cancer. Nature 487: 330-337, 2012.
53. Cancer Genome Atlas Research Network: Comprehensive molecular characterization of gastric adenocarcinoma. Nature 513: 202-209, 2014.
54. Cancer Genome Atlas Research Network; Analysis Working Group: Asan University; BC Cancer Agency; Brigham and Women's Hospital; Broad Institute; Brown University; Case Western Reserve University; Dana-Farber Cancer Institute; Duke University; Greater Poland Cancer Centre, *et al*: Integrated genomic characterization of oesophageal carcinoma. Nature 541: 169-175, 2017.
55. Shao Y, Jia H, Huang L, Li S, Wang C, Aikemu B, Yang G, Hong H, Yang X, Zhang S, *et al*: An original ferroptosis-related gene signature effectively predicts the prognosis and clinical status for colorectal cancer patients. Front Oncol 11: 711776, 2021.
56. Chatterjee S and Burns TF: Targeting heat shock proteins in cancer: A promising therapeutic approach. Int J Mol Sci 18: 1978, 2017.
57. Wu J, Liu T, Rios Z, Mei Q, Lin X and Cao S: Heat shock proteins and cancer. Trends Pharmacol Sci 38: 226-256, 2017.
58. Sun X, Ou Z, Xie M, Kang R, Fan Y, Niu X, Wang H, Cao L and Tang D: HSPB1 as a novel regulator of ferroptotic cancer cell death. Oncogene 34: 5617-5625, 2015.
59. Garrido C, Brunet M, Didelot C, Zermati Y, Schmitt E and Kroemer G: Heat shock proteins 27 and 70: Anti-apoptotic proteins with tumorigenic properties. Cell Cycle 5: 2592-2601, 2006.
60. Cheng J, Lv Z, Weng X, Ye S, Shen K, Li M, Qin Y, Hu C, Zhang C, Wu J and Zheng S: Hsp27 acts as a master molecular chaperone and plays an essential role in hepatocellular carcinoma progression. Digestion 92: 192-202, 2015.
61. Liu CL, Chen SF, Wu MZ, Jao SW, Lin YS, Yang CY, Lee TY, Wen LW, Lan GL and Nieh S: The molecular and clinical verification of therapeutic resistance via the p38 MAPK-Hsp27 axis in lung cancer. Oncotarget 7: 14279-14290, 2016.
62. Oesterreich S, Weng CN, Qiu M, Hilsenbeck SG, Osborne CK and Fuqua SA: The small heat shock protein hsp27 is correlated with growth and drug resistance in human breast cancer cell lines. Cancer Res 53: 4443-4448, 1993.
63. Shimada T, Tsuruta M, Hasegawa H, Okabayashi K, Shigeta K, Ishida T, Asada Y, Suzumura H, Koishikawa K, Akimoto S and Kitagawa Y: Heat shock protein 27 knockdown using nucleotide-based therapies enhances sensitivity to 5-FU chemotherapy in SW480 human colon cancer cells. Oncol Rep 39: 1119-1124, 2018.
64. Liang HH, Huang CY, Chou CW, Makondi PT, Huang MT, Wei PL and Chang YJ: Heat shock protein 27 influences the anti-cancer effect of curcumin in colon cancer cells through ROS production and autophagy activation. Life Sci 209: 43-51, 2018.
65. Hayashi R, Ishii Y, Ochiai H, Matsunaga A, Endo T, Hasegawa H and Kitagawa Y: Suppression of heat shock protein 27 expression promotes 5-fluorouracil sensitivity in colon cancer cells in a xenograft model. Oncol Rep 28: 1269-1274, 2012.
66. Ishida T, Ishii Y, Tsuruta M, Okabayashi K, Akimoto S, Koishikawa K, Hasegawa H and Kitagawa Y: Cetuximab promotes SN38 sensitivity via suppression of heat shock protein 27 in colorectal cancer cells with wild-type RAS. Oncol Rep 38: 926-932, 2017.
67. Liu Z, Liu Y, Long Y, Liu B and Wang X: Role of HSP27 in the multidrug sensitivity and resistance of colon cancer cells. Oncol Lett 19: 2021-2027, 2020.
68. Yang WS and Stockwell BR: Synthetic lethal screening identifies compounds activating iron-dependent, nonapoptotic cell death in oncogenic-RAS-harboring cancer cells. Chem Biol 15: 234-245, 2008.
69. Yang WS, SriRamaratnam R, Welsch ME, Shimada K, Skouta R, Viswanathan VS, Cheah JH, Clemons PA, Shamji AF, Clish CB, *et al*: Regulation of ferroptotic cancer cell death by GPX4. Cell 156: 317-331, 2014.
70. Dixon SJ, Winter GE, Musavi LS, Lee ED, Snijder B, Rebsamen M, Superti-Furga G and Stockwell BR: Human haploid cell genetics reveals roles for lipid metabolism genes in nonapoptotic cell death. ACS Chem Biol 10: 1604-1609, 2015.
71. Zhang X, Ma Y, Ma J, Yang L, Song Q, Wang H and Lv G: Glutathione peroxidase 4 as a therapeutic target for anti-colorectal cancer drug-tolerant persister cells. Front Oncol 12: 913669, 2022.
72. Benson AB, Venook AP, Al-Hawary MM, Arain MA, Chen YJ, Ciombor KK, Cohen S, Cooper HS, Deming D, Farkas L, *et al*: Colon cancer, version 2.2021, NCCN clinical practice guidelines in oncology. J Natl Compr Canc Netw 19: 329-359, 2021.
73. Hashiguchi Y, Muro K, Saito Y, Ito Y, Ajioka Y, Hamaguchi T, Hasegawa K, Hotta K, Ishida H, Ishiguro M, *et al*: Japanese Society for Cancer of the Colon and Rectum (JSCCR) guidelines 2019 for the treatment of colorectal cancer. Int J Clin Oncol 25: 1-42, 2020.
74. Yamazaki K, Yamanaka T, Shiozawa M, Manaka D, Kotaka M, Gamoh M, Shiomi A, Makiyama A, Munemoto Y, Rikiyama T, *et al*: Oxaliplatin-based adjuvant chemotherapy duration (3 vs. 6 months) for high-risk stage II colon cancer: The randomized phase III ACHIEVE-2 trial. Ann Oncol 32: 77-84, 2021.